Engineering Notes

ENGINEERING NOTES are short manuscripts describing new developments or important results of a preliminary nature. These Notes cannot exceed 6 manuscript pages and 3 figures; a page of text may be substituted for a figure or vice versa. After informal review by the editors, they may be published within a few months of the date of receipt. Style requirements are the same as for regular contributions (see inside back cover).

Holographic Structural Control for Large Space Reflectors and Radio Telescopes

T. A. HEPPENHEIMER*
Rockwell International, Downey, Calif.

Introduction

THE Power Relay Satellite (PRS) concept may transmit electric power via a 10-cm microwave beam, reflected off a satellite in geosynchronous orbit.[1] The satellite involves a reflecting surface 1 km in aperture with rms surface tolerance of 1.2 mm.[2] Also, the Satellite Solar Power Station (SSPS) requires the equivalent of a microwave antenna of 1 km aperture with rms surface tolerance of 2.5 mm. It is proposed to meet this requirement with an adaptive phased array constructed of slotted waveguide and fed by some 10^6 microwave generators (amplitrons).[3] In principle, a far simpler system involves a few high-power amplitrons feeding a paraboloidal antenna with the stated surface requirements.

To indicate the difficulty of constructing such surfaces, there is the q-index.[4] Let ε be the rms surface tolerance and D the aperture; then

$$q = \log_{10} D/\varepsilon \tag{1}$$

$q = 5.6$ for the SSPS, and 5.9 for the PRS. By contrast, large precision radio-telescopes such as Goldstone, Haystack, and Lebedev, representing the limit of the state-of-the-art, have $q = 4.6$–4.7.[2] Thus, the SSPS and PRS represent order-of-magnitude improvements over the present state-of-the-art. In radio telescopes, the loads producing deformation arise from gravity, winds, and thermal expansion. In the cited large space reflectors, the loads—much less severe—arise from gravity gradients and power beam or solar radiation pressures, as well as from thermal expansion. But the moment arms for these loads are so long that design of such reflectors still represents a difficult problem. In any event, the complex and heavy truss structures of radio telescopes are poorly suited to space applications.

Holographic Closed-Loop Surface Control

A reflector of conventional design may be regarded as an open-loop control system. The loads upon the structure constitute the inputs, the structural rigidity is the gain, and the deformation is the output. By decreasing the gain (strengthening the structure), one achieves the desired rms tolerance.

An alternate approach involves a lighter, more flexible structure which thus is subject to larger deformations. The surface proper is designed as an array of rigid elements, corner-mounted upon actuators, and supported by the light structure. The actuators translate the elements, within limits derived from the limits on structural deformation under load. Thus, by controlled translation, a precisely contoured surface is obtained. If the basic structure of a 1-km reflector is designed to achieve $\varepsilon = 1$ m, then $q = 3.0$ only. Worm-wheel actuators then can contour the surface to $\varepsilon = 0.1$ cm, for $q = 6.0$.

Received January 25, 1974; revision received February 25, 1974.
Index categories: Earth Satellite Systems, Unmanned; Spacecraft Configurational and Structural Design (Including Loads).

* Member of the Technical Staff, Space Division. Member AIAA.

To implement the actuator commands using a closed-loop control system, one requires a definition of the nominal surface contour. This can be provided using a computer-generated reference hologram.[5,6] At any time, information on the actual surface contour is given by a hologram of the surface. When this surface hologram and the reference hologram are superimposed and illuminated by laser, there results an image of the surface crossed by interference fringes. These fringes show the deviation from nominal of any point on the surface. If the surface center is defined as nominal, then since the fringes are equivalent to contours of constant deviation, fringe-counting immediately defines the deviation of any point. This fringe-counting can be done by computer, which thus derives commands for the individual actuators (Fig. 1).

Either microwave or optical holography may be used. In either case, however, hologram reconstruction or image formation is performed at optical wavelengths with a laser.[7]

The reference hologram is a computer plot of the Fourier transform of the wavefront associated with a mathematically-defined simple surface. To avoid ambiguity in the fringed-image interpretation, one should bias the reference surface curvature so that all displacements are positive. Thus, an appropriate reference surface is a spherical cap of very slight curvature; the nominal fringe pattern then is given by Newton's rings.

In applying microwave holography, one uses a stable frequency source driven by an oscillator with stability of one part in 10^7 or better; quartz oscillators can readily supply this stable, low-bandwidth (BW < 100 kHz) signal. This signal is fed into a power divider with horns so as both to illuminate the reflector surface and to provide a reference beam to the detector. The illumination scattered and reflected from the surface back to the detector then optically interferes with the reference beam; the resulting interference pattern defines the surface hologram.

The detector may be a two-dimensional array of horn receivers or dipoles, each matched into a preamplifier channel, or a single horn scanned in a raster pattern. The received signal is frequency-filtered, amplified, and used to modulate a CRT output, generating an optical display which is recorded on film.[8]

The surface hologram is constructed at microwave wavelength $\lambda = \varepsilon$, the desired resolution in rms surface roughness, such that each interference fringe in the surface image defines a surface deviation contour of $n\varepsilon$, n = fringe number. The image resolution is poor because of the use of finite detector elements. However, it is entirely adequate to have resolution comparable to the characteristic dimensions of the reflector surface panels (e.g., 10 m), so that the microwave holographic method is suitable.[9]

In applying optical holography, one cannot use holographic interferometry, since the fringe spacing (contour spacing) would

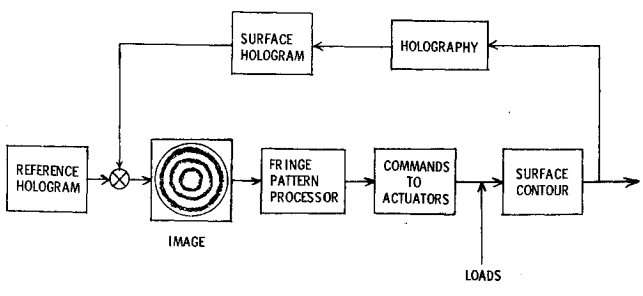

Fig. 1 The closed-loop system that controls the surface contour.

be $<1\,\mu$, which is three orders of magnitude too fine. Instead, one uses the "two-frequency" method[10]: one illuminates the surface with coherent light at two wavelengths, λ_1 and λ_2, such that $\varepsilon = \lambda_1\lambda_2/(\lambda_2 - \lambda_1)$. These two frequencies interfere to produce beats, such that the surface hologram, when reconstructed, gives an image crossed by fringes with spacing ε. These fringes, however, represent contours of constant range from the source, and not of constant deviation from the reference surface.

Thus, the reference hologram must also be computer-constructed with the same two wavelengths. Then, when reference hologram and surface hologram are superimposed and illuminated for image reconstruction, the image will contain two sets of range-contour fringes. These sets, in turn, will act to form a Moiré pattern, which is the interference pattern giving directly the desired contours of constant deviation.

The laser, analogous to the microwave source described above, must generate a line of width ~ 0.1 Å for adequate coherence.[11] A Fabry-Perot etalon permits operation in the two modes, λ_1 and λ_2. At the detector, a thin-film interference filter excludes ambient light at other wavelengths. An image intensifier amplifies the resulting light pattern, which is recorded on film as the surface hologram.

System Considerations

Consider now the derivation of power and bandwidth required to obtain the surface hologram, using microwave or optical methods.

In microwave holography, the bandwidth is set by the requirement that the illumination be coherent over the entire surface of the reflector, with characteristic length D. Thus, D must not exceed the coherence length L of the illumination, defined by

$$L = c/\Delta\nu \tag{2}$$

where c = speed of light and $\Delta\nu$ = allowable bandwidth. For $D = 1$ km, $\Delta\nu = c/D \sim 10^5$ Hz. This result is independent of λ.

In optical holography using the two-frequency method, the appropriate coherence length is set not by the object dimensions but by the range contour fringe spacing ε.[11] For $\varepsilon = 0.1$ cm, $\Delta\nu = c/\varepsilon = 3\times 10^{11}$ Hz so that laser linewidths of 0.1 Å, readily available, are entirely adequate.

In microwave holography, the required power may be given if it is assumed that the reflector surface is composed of resolution elements, each of which scatters or reflects enough radiation to be detectable with specified signal-to-noise ratio. Such resolution elements must be no larger than the surface panel elements. Then, let the following be given: N is the number of resolution elements in surface; r, the mean distance of detector from surface (m); T, the detector noise temperature (°K); $\Delta\nu$, the bandwidth (Hz); S/N, the desired signal-to-noise ratio (db); D, the aperture of detector element (cm); and α, the surface reflectance. Then, the required power of the microwave illumination is given by[12]

$$P = 4.17\times 10^{-18}[(Nr^2T\Delta\nu/D^2\alpha)\cdot 10^{(S/N)/10}]\text{ watts} \tag{3}$$

For example, let $N = 1000$, $r = 10^3 m$, $T = 150$°K, $\Delta\nu = 10^5$ Hz, $D = 0.2$ cm, $\alpha = 0.1$,† and $S/N = 20$ db. Then $P = 1570$ w. Thus, the microwave-holography method of surface control appears practical for even the largest reflectors.

Now consider the use of optical holography. The prime concern here is the noise due to solar illumination of the surface, some 1000 w/m^2 in the range 3500–7000 Å. The detector itself can be mounted off-axis such that it never sees the sun (or earth or moon), but it will see sunlight reflected and scattered off the reflector surface.

Narrow-passband interference filters, such as those used in solar observations, are available with passband $\leqq 0.5$ Å, transmissivity 10%. For a signal-to-noise ratio of only 10 db, then, the laser illumination of the surface must be ~ 1.0 w/m^2. Hence the laser power is at least comparable to the reflector area in m^2 (10^6w for a 1 km^2 reflector).

This implies the use of a pulsed laser, since continuous-wave (cw) lasers are incapable of such power levels. The energy in the pulse can be computed readily if one uses this criterion: that one photon shall be received per square wavelength of detector area, scattered or reflected from the surface. It is assumed that a telescope of aperture D_t focuses light upon an image-intensifier or detector of quantum efficiency η, diameter D_d. The transmissivity of the optics is τ_0. The reflector surface has area A, reflectivity α, and subtends solid angle Ω. Then, the energy E required in the pulse is

$$E = (hc/\lambda^3)(D_d/D_t)^2 A\cdot 2\pi/\eta\tau_0\,\alpha\Omega \tag{4}$$

where h is Planck's constant. For $\lambda = 0.5\mu$, $A = 1$ km^2, $\Omega = 1$ steradian, $\eta = 0.9$[13], $\tau_0 = 0.1$, $\alpha = 0.1$, and $(D_t/D_d) = 3$, we have $E = 124$ joules. This is well within the capabilities of modern advanced pulsed lasers, with pulse duration ~ 30 nsec.

However, for large reflectors, the two-frequency laser hologram method would be limited in applicability by the quality of photographic systems. To accurately record range contour fringes of spacing ε, over a surface of diameter D, requires a photographic record of (D/ε) resolution elements, or 10^{12} resels for $D = 1$ km, $\varepsilon = 0.1$ cm. Hence the two-frequency method may be limited to small systems, such as radio telescopes.

Radio Astronomy Applications

These methods of holographic control also can be applied to radio telescopes. Working with millimeter waves, for $\varepsilon = 0.1$ cm, it may be possible to raise the q-indices of the Parkes and Jodrell Bank instruments from 4.0 to above 4.5, while that of Arecibo could go from 4.0 to 5.0.

Atmospheric absorption renders impractical the use of wavelengths shorter than some 0.1 cm in microwave holography; optical wavelengths must be used. Thus the two-frequency method could readily be implemented, with modest pulse energies, to improve the performance of other existing radio telescopes. In principle, q-index values of 5.0–6.0 might be achieved, permitting effective radio astronomy at millimeter wavelengths. A new spectral band, an order of magnitude shorter than the presently observed centimeter band, would thus be opened to routine astronomical observations with existing instruments.

Conclusions

An active control system based on existing holographic technology has been proposed for maintaining the precision contours of large space reflectors. Such a system may employ either microwave holography or the two-frequency method in optical holography. This control method may also be applied to improve the performance of radio telescopes.

References

[1] Ehricke, K. A., "Regional and Global Energy Transfer via Passive Power Relay Satellites," SD 73-SH-0117, April 1973, Space Div., Rockwell International, Downey, Calif.

[2] Love, A. W., "Large Antennas for Microwave Power Transmission via Relay Satellite," IR & D 5235, Aug. 1973, Space Div., Rockwell International, Downey, Calif.

[3] Glaser, P. E., "Solar Power via Satellite," *Astronautics and Aeronautics*, Vol. 11, No. 8, Aug. 1973, pp. 60–68.

[4] Blevis, B. C., Day, J., Dohoo, R., and Roscoe, D., "Some Considerations in Satellite Communications Systems," Rept. 1122, Jan. 1964, Defence Research Telecommunications Establishment, Ottawa, Canada.

[5] Huang, T. S., "Digital Holography," *Proceedings of the IEEE*, Vol. 59, Sept. 1971, pp. 1335–1346.

[6] MacGovern, A. J. and Wyant, J. C., "Computer Generated Holograms for Testing Optical Elements," *Applied Optics*, Vol. 10, 1971, pp. 619–624.

[7] Cutrona, L. J., Leith, E. N., Porcello, L. J., and Vivian, W. E., "On the Application of Coherent Optical Processing Techniques to Synthetic Aperture Radar," *Proceedings of the IEEE*, Vol. 54, Aug. 1966, pp. 1026–1032.

† A mesh reflector may be very reflective at $\lambda = 10$ cm, but to detect $\varepsilon = 0.1$ cm one must use $\lambda = 0.1$ cm. At that wavelength, a mesh reflector may be nearly transparent.

[8] Larson, R. W., Zelenka, J. S., and Johansen, E. L., "Microwave Hologram Radar Imagery," *Proceedings of the Engineering Applications of Holography Symposium*, Society of Photo-Optical Instrumentation Engineers, Los Angeles, Calif., Feb. 16–17, 1972, pp. 3–18.

[9] Papi, G., Russo, S., and Sottini, S., "Microwave Holographic Interferometry," *IEEE Transactions on Antennas and Propagation*, Vol. AP-19, No. 6, Nov. 1971, pp. 740–746.

[10] Hildebrand, B. P. and Haines, K. A., "The Generation of Three-Dimensional Contour Maps by Wavefront Reconstruction," *Physics Letters (Netherlands)*, Vol. 21, No. 4, 1966, pp. 422–423.

[11] Wuerker, R. F., private communication, 1973, Redondo Beach, Calif.

[12] Harney, E. D., "Space Planners Guide," *USAF Systems Command*, 1965, p. III-39.

[13] Metz, W. D., "Television-Type Sensors for Astronomy: New Pictures," *Science*, Vol. 181, Sept. 7, 1973, pp. 930–931.

Testing the External Burning Propulsion Concept

H. L. Fein* and D. E. Shelor†
Atlantic Research Corporation, Alexandria, Va.

Introduction

Theoretical analysis[1] has indicated that external burning propulsion using the exhaust from a solid propellant as the fuel may offer performance superior to a conventional rocket in certain applications. In this propulsion concept, shown schematically in Fig. 1, the exhaust from a fuel-rich solid propellant is injected transversely through the vehicle boundary layer into the supersonic airstream surrounding the separation bubble at the vehicle base. There mixing and supersonic combustion occur, and the resulting pressure rise is transmitted to the vehicle base through the subsonic portion of the near wake. The analysis of Strahle[1] indicates that base pressures greater than the freestream static pressure are achievable.

Because of the encouraging analytical results, the authors undertook the experimental evaluation of this external burning propulsion concept. The purpose of this Note is to describe the testing techniques employed and to indicate testing considerations which are unique either to the propulsion concept or to the testing configuration.

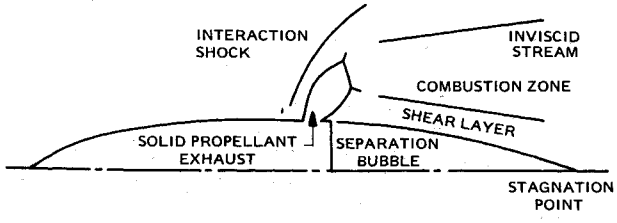

Fig. 1 Schematic diagram of the external burning propulsion concept.

Test Configuration

The ideal test configuration for this propulsion concept is probably a circular annular nozzle in which the base of the centerbody serves as the model of the vehicle base. However, as described below, the ratio of the nozzle diameter to the centerbody diameter should be as large as possible to eliminate interference effects. Thus, for the model sizes of interest, this configuration in full scale requires air flow rates not generally available except in the largest aerodynamic test facilities. Reduced scale models would probably be acceptable for a purely aerodynamic study, where interaction distances scale with model radius. However, for external burning, the combustion zone length is a second characteristic length, and the ratio of this length to the model radius strongly influences performance. If chemical reaction rates, as opposed to mixing rates, determine the length of the combustion zone, then the above ratio will not scale with model radius, and the results from reduced scale models could be misleading. Accordingly, a semiannular half model was selected to allow the maximum width of the annular air flow passage without reducing the scale of the model.

A diagram of the half-model configuration is shown in Fig. 2. During a test, air flows from the air supply through the nozzle, around the model section, and into the enclosed freejet test section. The fuel, i.e., the fuelrich exhaust from the solid propellant rocket motor mounted external to the test section, is injected into the airstream from the model just downstream of the point where the air enters the test section. The fuel mixes and burns with the air flow in the test section, and the combined flow then passes from the test section into the variable area diffuser. From the diffuser, the air exhausts to the atmosphere. For tests conducted at atmospheric freestream pressure, the freejet enclosure and diffuser are not needed, and the air/fuel mixture exhausts directly to the atmosphere.

The advantages of the half-model configuration over the full model are numerous. First, the required air flow rate is halved. Second, the fuel supply can be mounted external to the model and test section, simplifying the design. Third, the measurement of pressure distributions in the wake downstream from the model is easily accomplished using pressure ports mounted on the base plate extension (see Fig. 2). These pressure distributions have greatly aided the interpretation of test results. Finally, the extraction of temperature and pressure data from the model is simplified.

A possible disadvantage of the half model configuration is that the boundary layer on the base plate extension might provide a communication path between the subsonic near wake and pressure fields further downstream from the base. If this were the case, we would expect to see differences between the base pressure and downstream pressure distribution measured with a half model and those measured with a full model. In Fig. 3, the base pressure and downstream pressure distribution measured with the half model configuration are compared to data obtained with a full model by Reid and Hastings.[2] Except at $x/r = 4$, the agreement between the two sets of data is very good, providing no indication that the boundary layer on the plate affects the test results.

Design Considerations

Proper design of the test configuration is critical. First, if there is a static pressure mismatch between the supersonic freestream and the ambient pressure surrounding the nozzle, either expansion waves or a shock wave will originate at the lip of the outer nozzle wall and run toward the wake. If these waves intersect the wake too near to the model base, they will influence the measured base pressure. This problem is illustrated in

Presented as Paper 73-1226 at the AIAA/SAE 9th Propulsion Conference, Las Vegas, Nev., November 5–7, 1973; submitted November 16, 1973; revision received February 28, 1974. This work was supported in part by the Naval Ordnance Systems Command, Naval Ordnance Station, Indian Head, under Contracts N00174-71-C-0139, N00174-72-C-0105, and N00174-73-C-0240; and in part by the Air Force Rocket Propulsion Laboratory under Contract F04611-72-C-0044.

Index categories: Airbreathing Engine Testing; Airbreathing Propulsion, Subsonic and Supersonic; Combustion in Gases.

* Staff Scientist, Solid Propellant Department. Member AIAA.
† Head, Experimental Physics, Applied Physics Department.